



Cite this: *Nanoscale*, 2020, **12**, 6744

# Molecular generation targeting desired electronic properties *via* deep generative models†

Qi Yuan,<sup>a</sup> Alejandro Santana-Bonilla,<sup>a</sup> Martijn A. Zwijnenburg<sup>b</sup> and Kim E. Jelfs<sup>id</sup>\*<sup>a</sup>

As we seek to discover new functional materials, we need ways to explore the vast chemical space of precursor building blocks, not only generating large numbers of possible building blocks to investigate, but trying to find non-obvious options, that we might not suggest by chemical experience alone. Artificial intelligence techniques provide a possible avenue to generate large numbers of organic building blocks for functional materials, and can even do so from very small initial libraries of known building blocks. Specifically, we demonstrate the application of deep recurrent neural networks for the exploration of the chemical space of building blocks for a test case of donor–acceptor oligomers with specific electronic properties. The recurrent neural network learned how to produce novel donor–acceptor oligomers by trading off between selected atomic substitutions, such as halogenation or methylation, and molecular features such as the oligomer's size. The electronic and structural properties of the generated oligomers can be tuned by sampling from different subsets of the training database, which enabled us to enrich the library of donor–acceptors towards desired properties. We generated approximately 1700 new donor–acceptor oligomers with a recurrent neural network tuned to target oligomers with a HOMO–LUMO gap <2 eV and a dipole moment <2 Debye, which could have potential application in organic photovoltaics.

Received 18th December 2019,  
Accepted 4th March 2020

DOI: 10.1039/c9nr10687a

[rsc.li/nanoscale](http://rsc.li/nanoscale)

## Introduction

The successful development of new functional molecules remains one of the most important challenges to be addressed, not only due to the vastness of the chemical space to be explored, but also given the level of specificity required in the targeted properties for each application. In many cases, serendipity has played a fundamental role in the discovery and production of new materials and molecules. Recently, there is growing interest in applying artificial intelligence (AI) to the discovery of novel functional molecules, particularly in the field of drug discovery, with the aim of both exploring larger chemical space and saving the time and cost involved in the experimental synthesis and characterisation of such molecules.<sup>1–4</sup>

The use of AI in material discovery generally falls into two categories. Firstly, predictive AI models, based upon supervised machine learning, are becoming more common in the use for

the computation of material properties, calculating the properties of interest at reasonable accuracy, but a fraction of the computational cost compared to widely used electronic structure calculations. Predictive AI models have been applied widely for material discovery tasks, including organic photovoltaics,<sup>5–8</sup> bioinspired hierarchical composites<sup>9</sup> and supercompressible polymers.<sup>10</sup> Secondly, there are generative models, which use unsupervised machine learning such that a model learns from a dataset and can then produce data of a similar format. This can be applied in chemistry to produce novel molecules from libraries of known molecules. Generative models have been reported mainly for drug or drug-like molecules,<sup>11</sup> with only limited application for other types of functional molecules, for example non-fullerene electron acceptors<sup>12</sup> and thermally conductive polymers.<sup>13</sup> Our study here focuses on developing deep generative AI models for the discovery of novel donor–acceptor oligomers with desired electronic properties with potential application as organic semiconductors.

Development of a deep generative model for material discovery can be divided into several tasks. The first task is to represent the molecules of interest in a way that is easy to be read and written by a computer. A standard representation of molecules is the simplified molecular-input line-entry system (SMILES), which encodes molecular graphs compactly as human-readable strings. The SMILES representations of molecules highly resemble that of natural language, where long

<sup>a</sup>Department of Chemistry, Molecular Sciences Research Hub, White City Campus, Imperial College London, Wood Lane, London, W12 0BZ, UK.

E-mail: [k.jelfs@imperial.ac.uk](mailto:k.jelfs@imperial.ac.uk); Tel: +44 (0)207 594 3438

<sup>b</sup>Department of Chemistry, University College London, 20 Gordon Street, London WC1H 0AJ, UK

†Electronic supplementary information (ESI) available. See DOI: 10.1039/C9NR10687A



Recent development and design of electronic donor-acceptors has attracted significant attention due to their application in organic light emitting diodes (OLEDs),<sup>21</sup> organic photovoltaics (OPVs),<sup>22</sup> and non-linear optical (NLO) materials.<sup>23</sup> The donor-acceptor oligomers need to be modified in order to obtain desired electronic properties.<sup>24,25</sup> For example, the optical gap of donor-acceptor oligomers usually needs to be

In this work, we have developed deep generative models for the generation of molecular libraries of donor-acceptor oligomers with preferred electronic properties using an RNN combined with TL. TL was required as the libraries of existent donor-acceptor oligomers are not of sufficient magnitude for training a robust RNN model. We explore whether the structural and electronic properties of the donor-acceptors can be learned *via* TL, and whether the chemical space of the training sets can be fully explored with the TL models. As a proof of concept, we targeted the chemical space of donor-acceptor oligomers with an optical gap, as approximated by the HOMO-LUMO gap, close to 2 eV and a dipole moment smaller than 2 Debye. These oligomers can potentially form organic semiconductor crystals offering alternatives to the traditional families of molecular candidates such as oligoacenes or benzothieno[3,2-*b*][1] benzothiophene derivatives. A low HOMO-LUMO gap, and by extension a low optical gap, ensures the generated oligomers are promising materials for organic photovoltaics, and a low dipole moment in the ground state is desired as it has been shown that this can help with directing self-assembly towards supramolecular arrangements that promote macroscopic properties such as charge-carrier mobility.<sup>33</sup> Our approach would be equally applicable to a focus on a different region of property space and we would note that for optoelectronic device applications such as OPVs and OLEDs, it is typical for there to be multiple material properties and device characteristics contributing to high performance, and these would need to be considered and appropriately weighted on a case-by-case basis. We discuss the challenges for further extension of the method in the discussion.

We present an overview of our approach for generating novel donor–acceptor oligomers with targeted electronic properties in Fig. 1. In the following sections, we will describe the origin

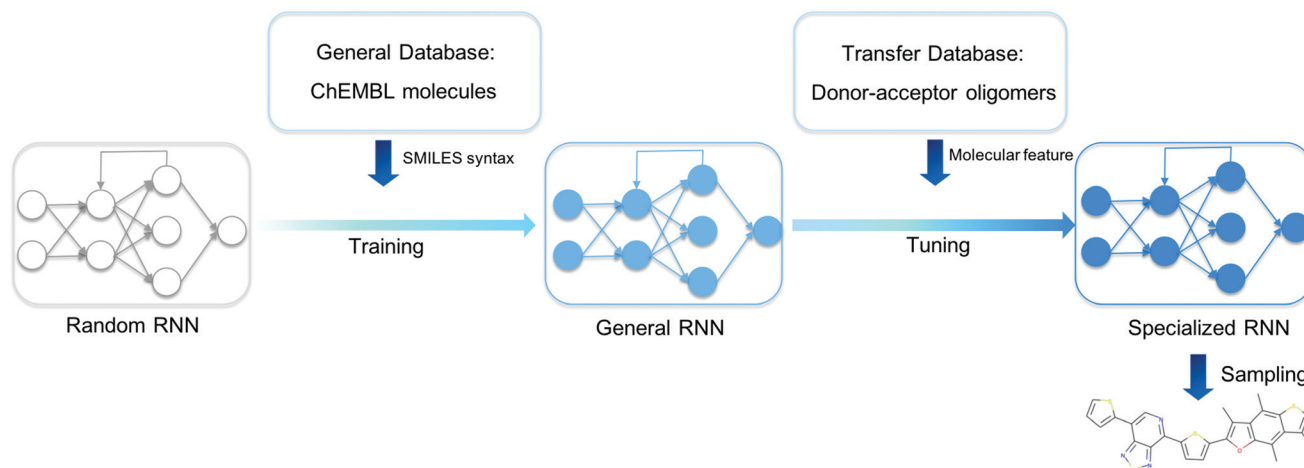


**Fig. 1** Our workflow for the discovery of novel donor–acceptor oligomers. An RNN with randomized parameters was built, and the General RNN was obtained by training the random RNN with the General Database of the ChEMBL library. The specialized RNN was developed by tuning the General RNN using the Transfer Database that only contains donor–acceptor oligomers, and then used to generate novel donor–acceptor oligomers.

of our datasets, how we first trained a general RNN and then used unsupervised cluster detection to uncover different clusters of molecules in a database of donor–acceptor oligomers. Next, we compared the performance of transfer learning models built from different transfer databases and finally validated the performance of the newly generated oligomers.

## Datasets

The task for molecular discovery using deep generative models can be divided into two parts; (i) learning the correct representation of molecules, for instance the valid SMILES representation, and (ii) learning the required structural property relationship of the molecules in order to generate novel functional molecules. To successfully carry out the first stage of the task, it is necessary to train the model on an extensive and varied database from which the syntax of valid SMILES can be learned. For the training of such an RNN model, which will hereafter be referred to as the ‘General RNN’, we used the GuacaMol Training SMILES database<sup>34</sup> as published by Brown *et al.*,<sup>35</sup> which contains 1.2 million SMILES string from the ChEMBL database. And we refer to the training set for the General RNN hereafter as the ‘General Database’. For the TL model, the ‘Database of organic donor–acceptor molecules’ from the Computational Materials Repository<sup>31</sup> was used and is referred to hereafter as the ‘Transfer Database’. The Transfer Database originally contained 5419 molecules, but after removing candidates that contained characters not present in the General Database and those for which density functional theory (DFT) calculations we carried out to characterise the molecular properties (see below) failed to converge, we were left with a final Transfer Database of 5024 molecules. The average length of the SMILES in the General Database is 47.6, while the average length of SMILES strings in the Transfer Database is 103.3, so it is of interest how well the General RNN

will be able to be applied to the more complex molecules in the Transfer Database.

The values of the Kohn–Sham HOMO–LUMO gaps, which we use to approximate the optical gaps, and dipole moments in the database of organic donor–acceptor molecules were previously calculated using the B3LYP functional.<sup>36–38</sup> However, due to the exponentially decaying nature displayed by this exchange–correlation, instead of the correct  $r^{-1}$  behaviour at long distances, the excitation energies can be expected to be underestimated and the polarizability overestimated.<sup>39,40</sup> We therefore performed additional calculations to evaluate the electronic properties of the oligomers in the Transfer Database with a long-range corrected DFT functional that does not suffer from this issue. Firstly, we generated 100 conformers of each oligomer using the RDKit ETKDG method<sup>41</sup> and evaluated the conformers’ energies using UFF.<sup>42</sup> The lowest energy conformation was then geometry optimised by using the GFN-xTB2 method as implemented in xTB.<sup>43</sup> The optimisation was considered complete when a threshold of  $8 \times 10^{-4}$  Hartrees per atomic unit length in forces and  $1 \times 10^{-6}$  Hartree in energies was reached, all conformations were confirmed to be true minima. We opted to optimise the geometry of the molecules using GFN-xTB2 rather than with DFT calculations due to the large number of molecules in the Transfer Database. A benchmark between geometries optimised using GFN-xTB2 and DFT ( $\omega$ B97X-D3/def2-TZVP) is reported in section 5 of the ESI,<sup>†</sup> showing that GFN-xTB2 provides reasonable geometries at a much reduced computational cost. The optical and electronic features such as the HOMO–LUMO gap and polarizabilities were then computed by employing the long-range corrected  $\omega$ B97X-D3 functional<sup>44</sup> as implemented in ORCA.<sup>45</sup> The ground and excited state properties were computed using the def2-TZVP basis set and by employing the simplified Tamm–Dancoff approach (sTDA).<sup>46–49</sup> Excited states with an excitation energy of lower than 10.0 eV were computed, corresponding to



approximately 300 singlet states and 300 triplet states. This methodology has been shown to produce reliable results in the case of co-polymers where optoelectronic properties have been computed and employed to train machine learning models.<sup>7</sup> Further analysis of the differences can be found in the ESI.† Our computational approach, using GFN-xTB first for geometries, cut the computational cost of obtaining structures and properties by a factor of about 3–4, with each molecule on average taking about 1 day to run on a 24-core node on a university supercomputer.

We found that now only 269 of the 5024 molecules in the 'Database of organic donor-acceptor molecules' were promising candidates for our target of an optical gap close to 2.0 eV and dipole moment smaller than 2.0 Debye, making them possible candidates for organic semiconductors. These results highlight the importance and need for TL to explore the chemical space, with the main objective of generating many more new molecules with the target properties.

### The General RNN model

The RNN architecture used in this paper is adapted from the work of Olivecrona *et al.*<sup>2</sup> The molecular SMILES were encoded to numeric vectors suitable for machine learning using 'one-hot' tokenization. In this study, there were 78 unique symbols in the SMILES strings of the Transfer Database. Two additional tokens, 'GO' and 'EOS' were added to each string to denote the beginning and end of a SMILES sequence. As a result, a SMILES string with  $n$  symbols was represented by an  $(n \times 80)$  dimensional vector. The specific RNN type used in this study was the Gated Recurrent Unit (GRU),<sup>50</sup> where each node in the RNN was designed to learn long range dependency within the SMILES string by keeping a weighted sum of information each character in the SMILES string possesses. Three stacked GRU layers were used to process the vectors generated from the SMILES strings in this study. The model was trained using the standard Adam optimizer, which is an extension of the gradient descent algorithm designed for the training of deep neural networks.<sup>51</sup> The generative RNN model in this work was implemented using Python 3.6 in combination with the PyTorch library.<sup>52</sup>

### Unsupervised cluster detection in the transfer database

In order to explore the chemical space of the Transfer Database, cluster detection within the Transfer Database was performed based upon their structural similarity. The Transfer Database was considered as a graph, where each molecule in the Transfer Database formed a node in the graph. The graph nodes were represented using the Morgan molecular fingerprints of the corresponding molecules. A Morgan fingerprint is a vector that indicates the presence of specific substructures within a molecule, and was computed here using the RDKit cheminformatics package.<sup>53</sup> The edges in the graph were defined using the pairwise Tanimoto similarities between the fingerprints of the molecules, which quantifies how similar a pair of molecular fingerprints are. In order to reduce the complexity of the graph, a cut-off of 0.25 was applied to the mole-

cular similarities, which means that molecules with similarity larger than 0.25 were considered 'connected' by an edge. The Louvain method<sup>54</sup> was applied to the graph to detect clusters within the Transfer Database; the method detects clusters by maximising the density of edges within each cluster compared to edges connecting different clusters. The Louvain modularity cluster detection was performed using Python 3.6. After the clusters were detected, the HOMO–LUMO gaps and dipole moments of molecules in each of the clusters were analysed to examine the shared properties of the clusters and determine the most suitable clusters for TL.

### Transfer learning

We wanted to examine whether using subsets of the Transfer Database that contained clusters of promising candidates with the desired properties would be a more effective way of generating new candidates with promising properties than using the entire Transfer Database for TL. Therefore, we carried out the cluster detection for the entire Transfer Database (5024 molecules) and separately for the set of 'promising' candidates (269 molecules). As a result, three subsets of both the Transfer Database and the 'promising' candidates were supplied to the General RNN for parameter fine-tuning, resulting in 6 TL models. The training sets for Models 1, 2 and 3 were subsets of the whole Transfer Database, while training sets for Models 4, 5 and 6 were subsets of the 269 'promising' candidates. All parameters in the General RNN were retrained during TL, with 15 epochs of training performed, which means that each of the TL models were fine-tuned by passing the corresponding training sets 15 times through the General RNN. 1024 SMILES strings were sampled from each epoch during the TL, resulting in 15 360 strings being generated from each TL model.

### Evaluating the transfer learning models

We evaluated the TL models by examining the validity, uniqueness and novelty<sup>35</sup> of the oligomer database generated by each model, as well as the ability of generating 'promising' molecules. The 'validity' measures the ability of the models to generate valid SMILE strings and was calculated by dividing the number of valid SMILES strings (as confirmed using the RDKit package) generated by each model over the total number of strings sampled by each model. The 'uniqueness' measures the ability of the model to generate unique SMILES that had not already been sampled and was calculated by dividing the number of unique SMILES generated over the number of valid SMILES generated by each model. The 'novelty' measures the models in terms of generating oligomers that were not already present in the training sets, and was calculated by dividing the number of valid and unique SMILES strings that were not already found in the corresponding training set over the total number of valid and unique SMILES generated by each model.

For each TL model, about 4000 novel molecules were generated, thus the computational cost of evaluating the electronic properties of all the 24 000 generated molecules using DFT was prohibitive. We estimated that this would have required approximately 24 000 days on 24-core nodes, which even with





access to massively parallel computer architectures, was not viable. Instead, to assess the properties of the generated molecules at acceptable computational cost, the HOMO–LUMO gaps and dipole moments were calculated using supervised gradient boosted decision tree (GBDT) models trained on the Transfer Database. The GBDT algorithm uses a weighted ensemble of decision trees to fulfill regression or classification tasks. The GBDT model was trained on the Transfer Database, with the database randomly divided into training (80%, 4019 molecules) and test (20%, 1005 molecules) sets, and the Morgan fingerprints calculated using RDKit as the molecular input feature. Morgan fingerprints with varied length (512, 1024, 2048) and radius (2, 4, 6) were used for the molecular fingerprinting. The GBDT models were optimised so as to minimise the mean squared error between the predicted values and the true values in the training set. The GBDT models were then used upon the generated unique and novel molecules from TL to predict their HOMO–LUMO gaps and dipole moments. Those molecules with a HOMO–LUMO gap less than 2 eV and dipole moment less than 2 Debye were deemed ‘promising’, as they were the target of our study. In order to validate the ‘promising’ molecules identified using the GBDT models, 90 ‘promising’ molecules were randomly sampled from the ‘promising’ generations and their HOMO–LUMO gaps and dipole moments were calculated using DFT calculations with the  $\omega$ B97X-D3 functional, using the setup as described above.<sup>44</sup>

## Results and discussion

### Supervised machine learning model of electronic properties

Supervised GBDT models were developed to evaluate the donor–acceptor oligomers generated from the generative RNNs. It was found in this study that a GBDT model using Morgan fingerprint with length 1024 and radius 2 had the lowest error in terms of predicting the properties of the oligomers in the test set. The comparison between the  $\omega$ B97X-D3-

calculated electronic properties and those predicted using the GBDT models on the test set (20% of the Transfer Database, 1005 molecules) is shown in Fig. 2. The mean absolute error of the GBDT prediction for HOMO–LUMO gaps is 0.09 eV and for dipole moments is 1.31 Debye. While the GBDT model is therefore reasonably accurately predicting the HOMO–LUMO gap of the molecules, the accuracy of the prediction for the dipole moments was significantly lower. Previously, graph neural network models using molecular graphs as feature vector inputs, such as the SchNet,<sup>55</sup> MEGNet<sup>56</sup> were trained to predict the dipole moments of functional molecules with good accuracy. However, when we tested these models for our study, the mean absolute error of the dipole moment predictions was exceptionally large (over 10 Debye). The poor performance of the graph neural networks on the Transfer Database was probably due to the fact that such models were trained and tested against the QM9 dataset,<sup>57</sup> which contains only molecules with no more than 9 heavy atoms. However, the number of heavy atoms in molecules in our Transfer Database ranges from 20 to 180, and application of such graph convolution networks was therefore inadequate due to the complexity of molecules in the Transfer Database. We trialled other models, such as random forest, and other fingerprints, such as Molecular Access System (MACCS) keys,<sup>58</sup> but these performed less well than our selected model.

Here, we aim to discover as many ‘promising’ oligomers as possible for further validation, thus recall (identifying ‘promising’ oligomers) was pursued at the sacrifice of precision (labelling ‘promising’ oligomers correctly). The mean error of GBDT prediction for dipole moment was 0 Debye, with a standard deviation of 1.83 Debye. The molecules generated *via* TL were fed into the GBDT models to predict their electronic properties. Molecules with a GBDT-predicted dipole moment of lower than 3.66 Debye (corresponding to 0.9 standard deviation above the mean error of 0 Debye) and a HOMO–LUMO gap lower than 2.0 eV were considered as potential ‘promising’ oligomers. The choice of 3.66 Debye as cutoff for ‘promising’ oligomers implies a higher false positive rate and lower false

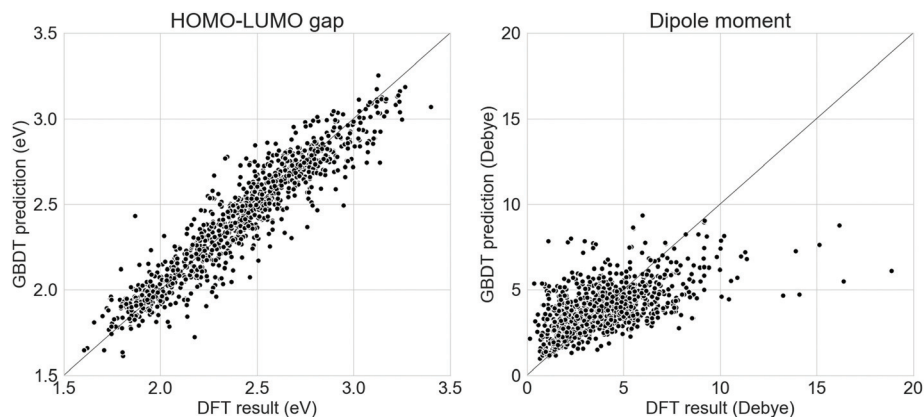
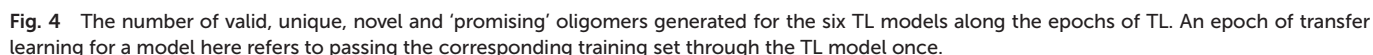


Fig. 2 Relationship between the DFT calculated electronic properties and GBDT predictions on the test set of the Transfer Database for (left) the HOMO–LUMO gap and (right) the dipole moment. The line of  $y = x$  is shown in both plots.



 CC BY-NC



In addition to learning the structural properties of the training sets, another task for the TL was to learn the electronic properties of the training molecules. Since the properties of the generated molecules were evaluated using the GBDT model and accurate prediction of dipole moment was not achieved in this study, only the HOMO–LUMO gaps were examined. The distributions of the HOMO–LUMO gaps of the molecules generated from the TL models at the 10th epoch are shown in Fig. 5(b) and shown for each epoch in Fig. S7.† For Models 4, 5 and 6, the HOMO–LUMO gaps of the vast majority

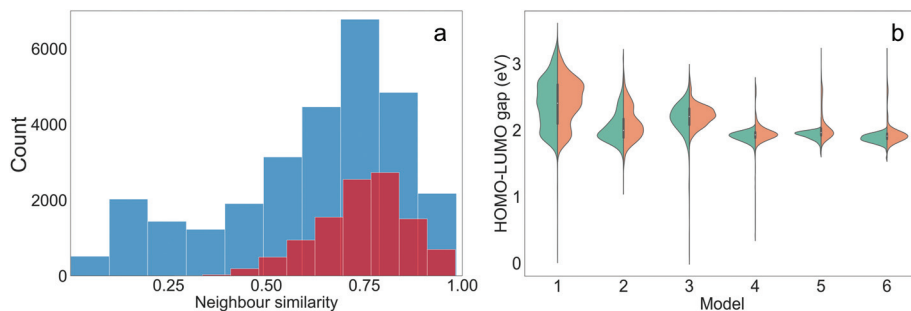


**Fig. 5** (a) Distribution of the neighbour similarities of all the generated oligomers (blue) and the 'promising' oligomers (maroon); (b) distribution of the HOMO–LUMO gaps of the molecules generated from the six TL models on the 10th epoch (red) compared to the corresponding training sets (green).

of generated molecules are lower than 2.0 eV, and therefore the chance of obtaining 'promising' oligomers increased. Models 1 through 6 had varied distributions of HOMO–LUMO gaps and all of these specific distributions were 'learned' by the corresponding TL models. Therefore, the HOMO–LUMO gaps of the generated molecules can be tuned by sampling different subsets of the training database of interest.

### Chemical space exploration

The ability for deep generative models to sample larger chemical space while obtaining oligomers with desirable properties is also important. This is a particular goal of the study here – to see whether our approach can move beyond traditional substitution strategies well established in the material chemistry community, to uncover 'wild cards' that might suggest alternative molecular replacements or a series of fragment alterations. The training sets of the TL models covered different regions of the chemical space, and it was expected that each of the models would cover the corresponding chemical space. In addition, covering chemical space beyond the training sets could lead to the discovery of novel donor–acceptor oligomers that had not been considered. To create a qualitative visualisation of the chemical space covered by the molecules in this study, the t-SNE projections of the fingerprints of the molecules generated from the six TL models, together with the fingerprints of the molecules in the corresponding training sets are shown in Fig. S8.† The chemical space of each training set has been thoroughly explored by the corresponding TL model, as well as unexpected regions of the chemical space of the training sets having also been covered, especially for Models 4, 5, and 6. It was thus possible to generate donor–acceptor oligomers that are not directly related to those in the Transfer Database from the TL models.

Merely covering more chemical space does not ensure the discovery of novel 'promising' donor–acceptor oligomers; it is possible that oligomers in the newly explored regions do not exhibit the preferred electronic properties. To compare the chemical space covered by the 'promising' oligomers, the t-SNE projections of only the 'promising' training and generated oligomers are shown in Fig. 6. Representative molecules were sampled from the 'promising' oligomers generated from

each TL model, and the structure of such molecules and their t-SNE projection values are shown in Fig. S9.† It can be seen from Fig. 6 that 'promising' oligomers generated from the TL explored well the corresponding chemical spaces of their respective training sets. As demonstrated in Fig. 6 and S9,† the 'promising' oligomers generated from Model 3 occupy a different region of chemical space compared to the other five models. In addition, oligomers generated from Models 5 and 6 occupied different sub-parts of the chemical space than Model 4. It is thus possible to explore particular regions of interest in chemical space by tuning the training sets for TL with the assistance of unsupervised cluster detection. However, the chemical spaces covered by the 'promising' oligomers were more conservative than that covered by all the generated molecules, as seen by higher neighbour similarity in Fig. 5a. The distribution of the neighbour similarities of generated molecules with their corresponding training sets for each of the TL models are shown in Fig. S10,† and the trend of 'promising' oligomers having higher neighbour similarities was found for all six models. Such results indicate that the excessive regions of chemical space explored by the TL models had limited contributions in terms of providing 'promising' oligomers, and the trade-off between exploring unseen regions of the chemical spaces and generating a greater percentage of more 'promising' oligomers is something to bear in mind.

The t-SNE projections in this study are the two-dimensional projection of the 1024-bit molecular fingerprints, allowing one to visualise the distribution of the high dimensional fingerprints. The computed neighbours in the t-SNE plots could result from either structural similarity (as intended) or from a crowding effect of the low dimensional representation of high dimensional data. Examples of 'promising' generated molecules with high and low similarity with their nearest neighbour in the training sets are shown in Fig. 7. A 'promising' oligomer with high similarity to a neighbour could be generated by simple atom replacement, while a 'promising' oligomer with a low similarity to a neighbour less than 0.6 involves multiple alterations on the neighbour molecule, which would be difficult to suggest by using traditional experimental functionalisation strategies. We obtained about 1300 'promising' oligomers with similarity to a neighbour lower than 0.6 with the





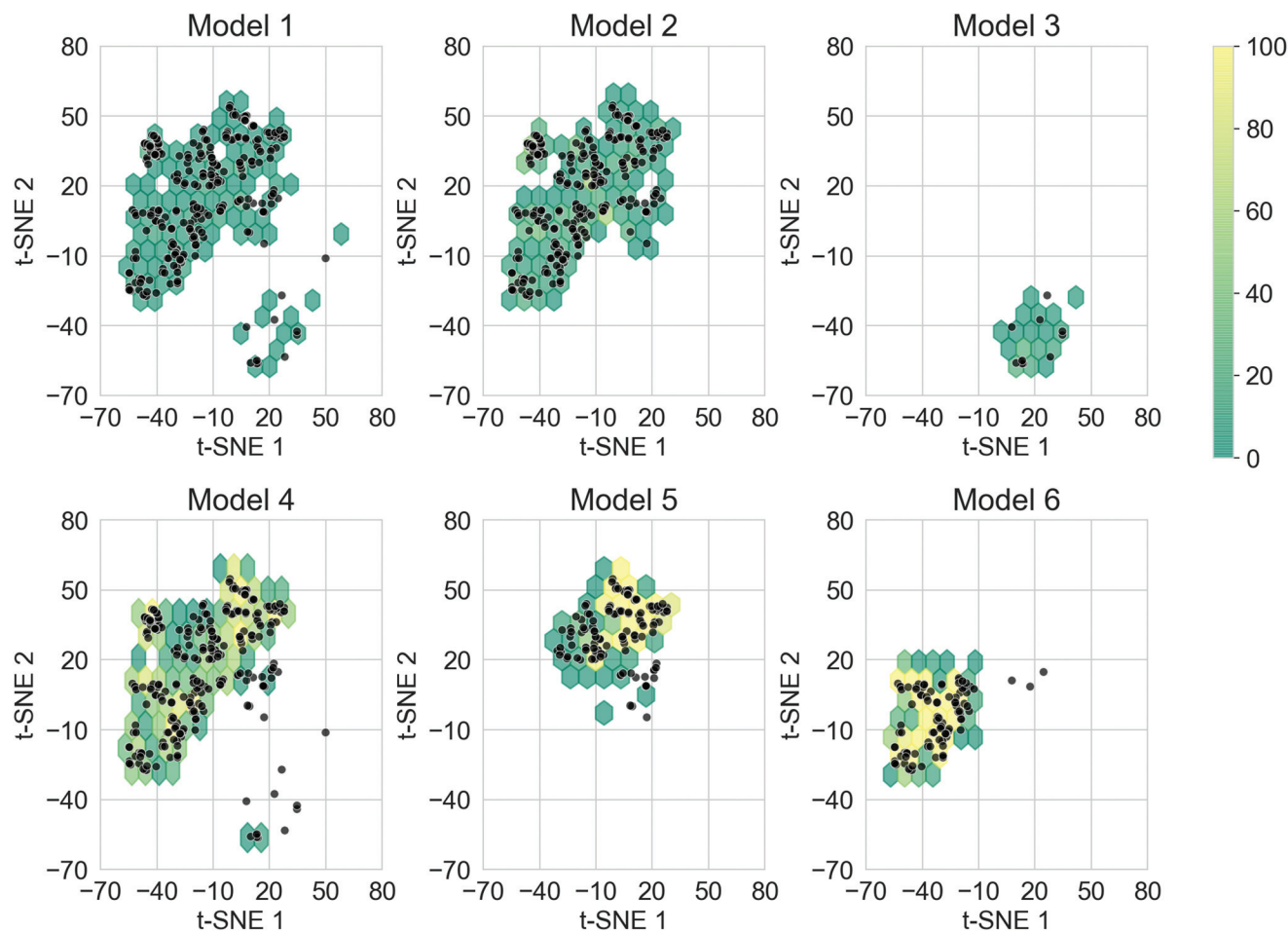


**Fig. 6** Hexagonal binning plot of the t-SNE projection of the fingerprints of the 'promising' molecules generated from the TL models. Colours of the hexagons represent the density of generated 'promising' oligomers in each hexagon according to the colour bar. The 'promising' molecules in the corresponding training sets are shown as black points. t-SNE 1 and t-SNE 2 correspond to the first and second dimensions of the 2-D projection of the molecular fingerprints.

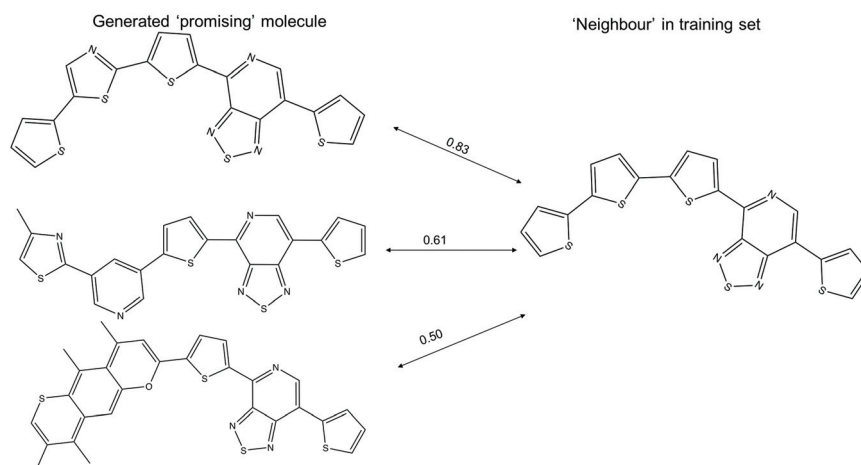


**Fig. 7** Example of three 'promising' oligomers generated from the TL and their nearest neighbour in the training set, as calculated using the Tanimoto similarity criterion. The Tanimoto similarities between the donor-acceptor oligomers are shown above the arrows. It should be noted that these 2-dimensional structures do not show the exact 3-dimensional conformation of the molecule used in the calculations.



Within the predicted structures, one can find known units, such as thiophene and furan, which have been previously used in the construction of donor-acceptor oligomers. The deep generative model also performed interesting substitutions such as fluorination or methylation. These strategies are commonly found in the literature and can be categorised as traditional substitutions in donor-acceptor oligomers. Similarly, completely changed small units such as selenophene (e.g. Fig. 8o) can be found within the set of suggested molecular transformations executed by the deep generative model. Analogously, one can observe frequently employed units for donor-acceptor molecules such as benzo[1,2-*b*:4,5-*b'*]dithiophene (BDT)<sup>62</sup> or pyridal[2,1,3]thiadiazole(PyT).<sup>63</sup> However, the original composition of the molecule is not preserved in all cases, with the molecules displaying interesting atomic substitutions in the core such as BDT selenium (Fig. 8i) or oxygen substituted (Fig. 8v). Similar molecules have been experimentally synthesised and characterised as organic semiconductor with enhanced charge-carrier mobility as a consequence of such replacements.<sup>64</sup> These previous findings provide an argument in favour of the capability of the deep generative model not only to offer an effective procedure to

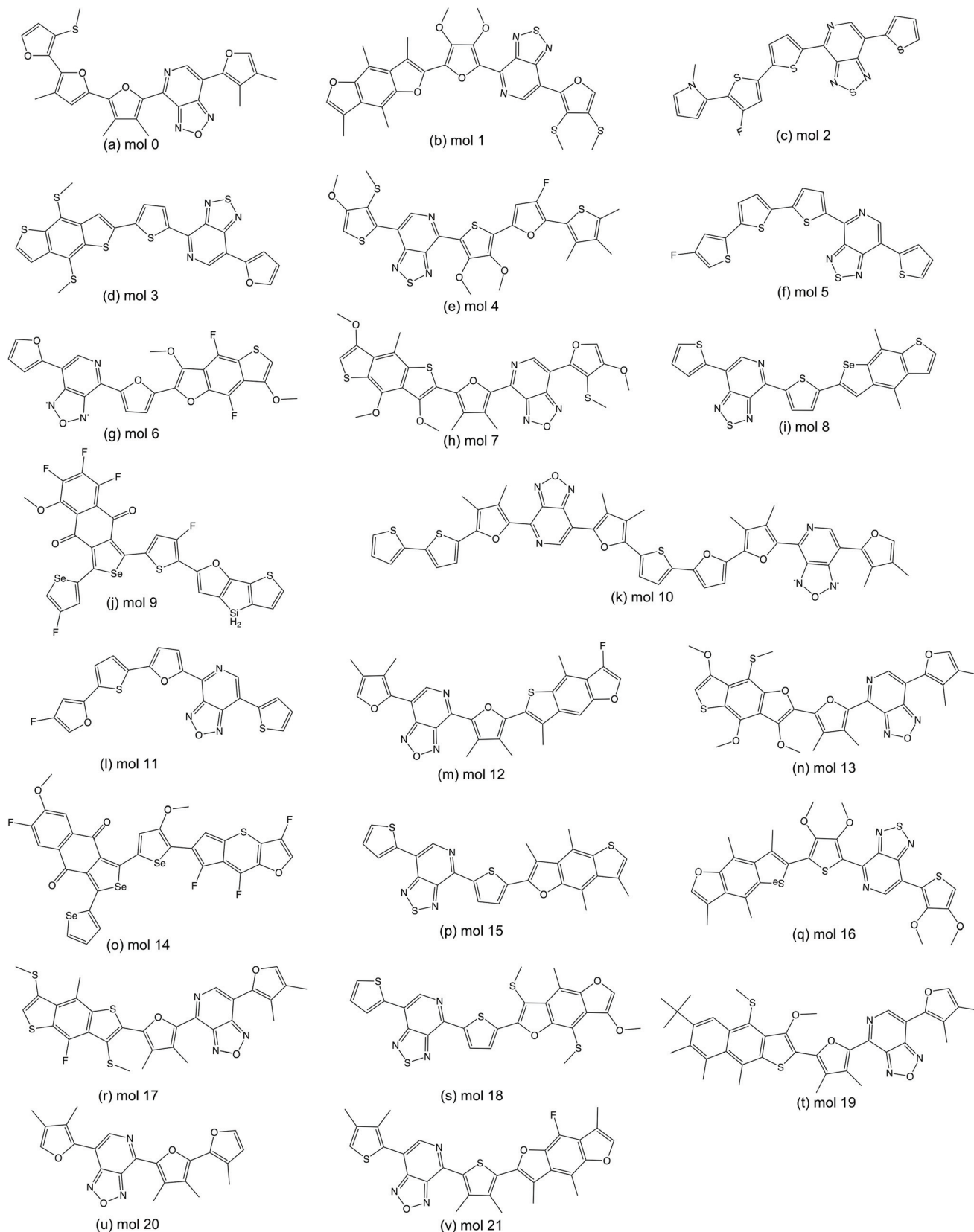
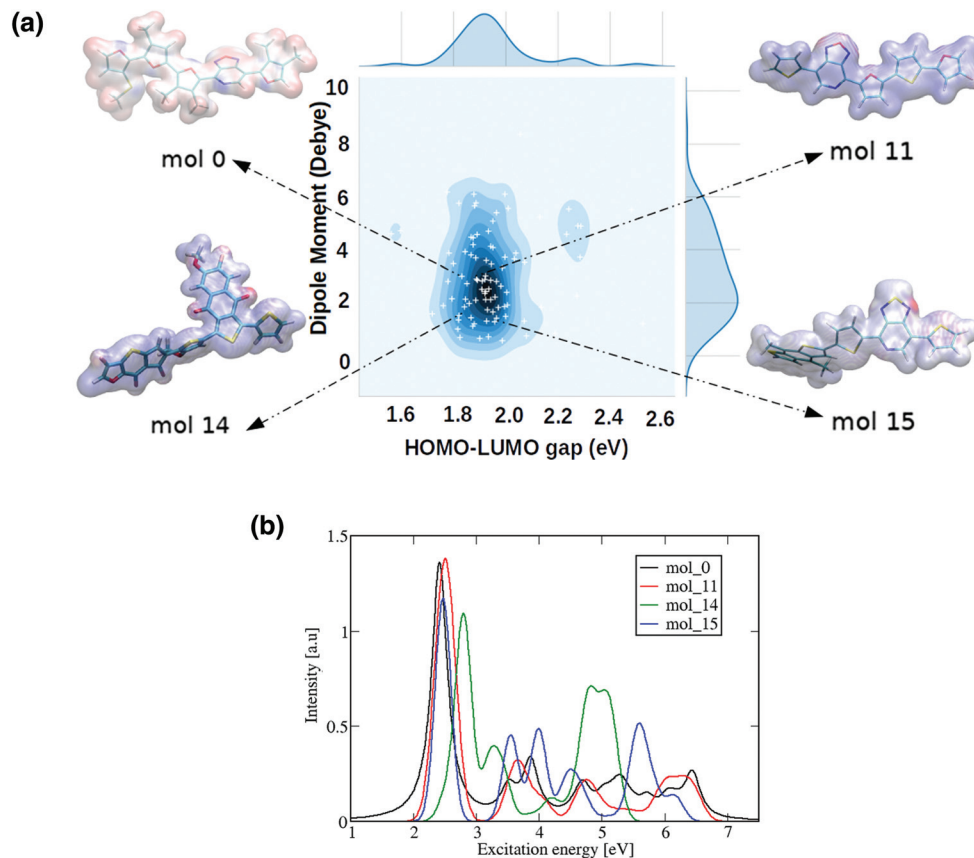


Fig. 8 The subset of 'promising' oligomers validated by DFT calculations.





**Fig. 9** (a) Distribution of the  $\omega$ B97X-D3 calculated HOMO–LUMO gaps and dipole moments of 90 randomly selected ‘promising’ oligomers generated from our trained deep generative model. Each newly produced donor–acceptor oligomer is represented as a white cross in the 2-D distribution, where darker regions represent a greater density of molecules found. The example molecules are shown with their molecular electrostatic potential, red represents more electron-rich regions and blue more electron-poor. (b) Computed UV-Vis spectra for the 4 selected oligomers.

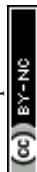
explore the chemical space, but also as a tool to provide new ideas and paths for novel atomic substitutions.

The TL model in this work is not limited to the generation of novel donor–acceptor oligomers as organic semiconductors; with proper tuning of the training sets for TL, electronic materials for other applications could be obtained. For example, the power conversion efficiency of organic solar cells is qualitatively related to HOMO energy of the donor, LUMO energy of the acceptor, and bandgap of the donor according to the Scharber model;<sup>65</sup> OLED materials require low singlet–triplet gap and minimized spatial overlap of HOMO and LUMO.<sup>66,67</sup> If such properties can be described with a supervised learning model from molecular information contained in the SMILES representation, the TL models can ‘learn’ the relevant properties with corresponding tuning of the training sets. In addition, when multiple electronic properties need to be optimized to improve device performance, the optimization can be assisted with a sampling approach such as an evolutionary algorithm (EA). In this fashion, we believe that the low precision and high recall model in discovering novel donor–acceptor oligomers can be used as a new methodology to discover and enhance selected families of new materials.

There are challenges in applying this type of approach to more complex properties beyond simple single molecule properties, particularly for applications based on combinations of properties. The first bottleneck to focus on to test expanding the approach is the generation of further training data for organic materials, such as to include excited state properties or, even more challenging, properties or behaviours beyond the single molecule level. While calculation of these properties *ab initio* for the requisite large number of systems is computationally demanding, it is pleasing to note recent additions to open-source databases in this area, which will open up new opportunities.<sup>32</sup> Of course, device characteristics that are not predominantly linked to molecular features, such as preparation conditions and sample history that influence the device microstructure, are beyond the scope of what could be screened for by this approach. However, identification of promising molecules is still an important starting point.

## Conclusions

In attempting to discover new molecular building blocks with promising properties for materials, a limitation can come





from the ability to truly explore and optimise the vast chemical space of possibilities. Here we have focused on an approach using recurrent neural networks (RNN) combined with transfer learning (TL) to effectively discover novel molecules with targeted properties for donor–acceptor oligomers. While most previously reported deep generative models for molecule discovery have focused on drug discovery, we showed that the generative models trained from a pharmaceutical database can be transferred to relatively large and complex systems such as the donor–acceptor oligomers. Different chemical and electronic property spaces were covered using different subsets of molecules as training sets. Both structural and electronic properties can be ‘learned’ through TL, thus the RNN models suggested in this study can be used to target different property spaces to fulfill the requirement of different types of electronic materials. Many of the molecular transformations learnt mimic those used to enhance performance in donor–acceptor systems in the literature. The models developed and the ‘promising’ oligomers identified are open to future theoretical and experimental validation.

An ideal generative model for molecular discovery would enable exploration of wider chemical space while retaining desired properties. However, it was found in this study that there is some degree of trade-off between exploration of chemical space and the optimisation of electronic properties. ‘Wild’ modifications to the training molecules were observed, likely modifications that would not be proposed by chemists, but such molecules did not generally exhibit satisfactory electronic properties. The generated ‘promising’ oligomers, with target properties, were more ‘conservative’ neighbours of the oligomers in the training set. The two factors need to be balanced in future molecular discovery tasks, although there is always the possibility that we are seeking a ‘needle in a hay stack’ – an extreme modification that still has the desired properties and has truly allowed us to move out of the region of chemical space that would be considered by chemists alone.

## Conflicts of interest

There are no conflicts to declare.

## Acknowledgements

We acknowledge funding from the European Research Council under FP7 (CoMMaD, ERC Grant No. 758370), and the Engineering Research Council and Physical Sciences Research Council (EPSRC) (EP/M017257/1, EP/P005543/1, EP/N004884/1), including the UK's HEC Materials Chemistry Consortium (EP/L000202/1) for time on the UK supercomputer, ARCHER. K. E. J. thanks the Royal Society for a University Research Fellowship. We thank Drs Andrew Tarzia, James Pegg and Liam Wilbraham for useful discussions.

## References

- 1 M. H. S. Segler, T. Kogej, C. Tyrchan and M. P. Waller, Generating Focused Molecule Libraries for Drug Discovery with Recurrent Neural Networks, *ACS Cent. Sci.*, 2018, **4**, 120–131.
- 2 M. Olivecrona, T. Blaschke, O. Engkvist and H. Chen, Molecular de-novo design through deep reinforcement learning, *J. Cheminf.*, 2017, **9**, 48.
- 3 D. Merk, F. Grisoni, L. Friedrich and G. Schneider, Tuning artificial intelligence on the de novo design of natural-product-inspired retinoid X receptor modulators, *Commun. Chem.*, 2018, **1**, 68.
- 4 R. Gómez-Bombarelli, J. N. Wei, D. Duvenaud, J. M. Hernández-Lobato, B. Sánchez-Lengeling, D. Sheberla, J. Aguilera-Iparraguirre, T. D. Hirzel, R. P. Adams and A. Aspuru-Guzik, Automatic Chemical Design Using a Data-Driven Continuous Representation of Molecules, *ACS Cent. Sci.*, 2018, **4**, 268–276.
- 5 S. A. Lopez, B. Sanchez-Lengeling, J. de Goes Soares and A. Aspuru-Guzik, Design Principles and Top Non-Fullerene Acceptor Candidates for Organic Photovoltaics, *Joule*, 2017, **1**, 857–870.
- 6 D. Padula, J. D. Simpson and A. Troisi, Combining electronic and structural features in machine learning models to predict organic solar cells properties, *Mater. Horiz.*, 2019, **6**, 343–349.
- 7 L. Wilbraham, R. Sprick, K. Jelfs and M. Zwijsburg, Mapping binary copolymer property space with neural networks, *Chem. Sci.*, 2019, **10**, 4973–4984.
- 8 P. B. Jørgensen, M. Mesta, S. Shil, J. M. García Lastra, K. W. Jacobsen, K. S. Thygesen and M. N. Schmidt, Machine learning-based screening of complex molecules for polymer solar cells, *J. Chem. Phys.*, 2018, **148**, 241735.
- 9 G. X. Gu, C.-T. Chen, D. J. Richmond and M. J. Buehler, Bioinspired hierarchical composite design using machine learning: simulation, additive manufacturing, and experiment, *Mater. Horiz.*, 2018, **5**, 939–945.
- 10 M. A. Bessa, P. Glowacki and M. Houlder, Bayesian Machine Learning in Metamaterial Design: Fragile Becomes Supercompressible, *Adv. Mater.*, 2019, 1904845.
- 11 D. C. Elton, Z. Boukouvalas, M. D. Fuge and P. W. Chung, Deep learning for molecular design—a review of the state of the art, *Mol. Syst. Des. Eng.*, 2019, **4**, 828–849.
- 12 B. Sanchez-Lengeling, C. Outeiral, G. L. Guimaraes and A. Aspuru-Guzik, Optimizing distributions over molecular space. An objective-reinforced generative adversarial network for inverse-design chemistry (ORGANIC), *ChemRxiv*, 2017, DOI: 10.26434/chemrxiv.5309668.v3.
- 13 S. Wu, Y. Kondo, M. Kakimoto, B. Yang, H. Yamada, I. Kuwajima, G. Lambard, K. Hongo, Y. Xu, J. Shiomi, C. Schick, J. Morikawa and R. Yoshida, Machine-learning-assisted discovery of polymers with high thermal conductivity using a molecular design algorithm, *npj Comput. Mater.*, 2019, **5**, 5.



- 14 T. Young, D. Hazarika, S. Poria and E. Cambria, Recent Trends in Deep Learning Based Natural Language Processing [Review Article], *IEEE Comput. Intell. Mag.*, 2018, **13**, 55–75.
- 15 N. Boulanger-Lewandowski, Y. Bengio and P. Vincent, Modeling Temporal Dependencies in High-dimensional Sequences: Application to Polyphonic Music Generation and Transcription, *Proceedings of the 29th International Conference on Machine Learning*, USA, 2012, pp. 1881–1888.
- 16 J. J. Irwin, T. Sterling, M. M. Mysinger, E. S. Bolstad and R. G. Coleman, ZINC: A Free Tool to Discover Chemistry for Biology, *J. Chem. Inf. Model.*, 2012, **52**, 1757–1768.
- 17 E. Jannik Bjerrum and R. Threlfall, Molecular Generation with Recurrent Neural Networks (RNNs), *arXiv e-prints*, 2017, <https://arxiv.org/abs/1705.04612>.
- 18 J.-L. Reymond, The Chemical Space Project, *Acc. Chem. Res.*, 2015, **48**, 722–730.
- 19 B. Sanchez-Lengeling and A. Aspuru-Guzik, Inverse molecular design using machine learning: Generative models for matter engineering, *Science*, 2018, **361**, 360–365.
- 20 I. Goodfellow, J. Pouget-Abadie, M. Mirza, B. Xu, D. Warde-Farley, S. Ozair, A. Courville and Y. Bengio, *Generative adversarial nets. Advances in neural information processing systems*, 2014, pp. 2672–2680.
- 21 Y. Tao, C. Yang and J. Qin, Organic host materials for phosphorescent organic light-emitting diodes, *Chem. Soc. Rev.*, 2011, **40**, 2943–2970.
- 22 A. Mishra and P. Bäuerle, Small molecule organic semiconductors on the move: promises for future solar energy technology, *Angew. Chem., Int. Ed.*, 2012, **51**, 2020–2067.
- 23 M. J. Cho, D. H. Choi, P. A. Sullivan, A. J. Akelahitis and L. R. Dalton, Recent progress in second-order nonlinear optical polymers and dendrimers, *Prog. Polym. Sci.*, 2008, **33**, 1013–1058.
- 24 G. S. He, L.-S. Tan, Q. Zheng and P. N. Prasad, Multiphoton Absorbing Materials: Molecular Designs, Characterizations, and Applications, *Chem. Rev.*, 2008, **108**, 1245–1330.
- 25 L. R. Dalton, P. A. Sullivan and D. H. Bale, Electric Field Poled Organic Electro-optic Materials: State of the Art and Future Prospects, *Chem. Rev.*, 2010, **110**, 25–55.
- 26 P. Kautny, F. Glöcklhofer, T. Kader, J.-M. Mewes, B. Stöger, J. Fröhlich, D. Lumpi and F. Plasser, Charge-transfer states in triazole linked donor–acceptor materials: strong effects of chemical modification and solvation, *Phys. Chem. Chem. Phys.*, 2017, **19**, 18055–18067.
- 27 S. K. M. Nalluri and R. V. Ulijn, Discovery of energy transfer nanostructures using gelation-driven dynamic combinatorial libraries, *Chem. Sci.*, 2013, **4**, 3699–3705.
- 28 Y. Li, T. Miao, P. Li and L. Wang, Photo-Driven Synthesis of C6-Polyfunctionalized Phenanthridines from Three-Component Reactions of Isocyanides, Alkynes, and Sulfinic Acids by Electron Donor–Acceptor Complex, *Org. Lett.*, 2018, **20**, 1735–1739.
- 29 A. Postigo, Electron Donor–Acceptor Complexes in Perfluoroalkylation Reactions, *Eur. J. Org. Chem.*, 2018, 6391–6404.
- 30 J. Hachmann, R. Olivares-Amaya, S. Atahan-Evrenk, C. Amador-Bedolla, R. S. Sánchez-Carrera, A. Gold-Parker, L. Vogt, A. M. Brockway and A. Aspuru-Guzik, The Harvard clean energy project: large-scale computational screening and design of organic photovoltaics on the world community grid, *J. Phys. Chem. Lett.*, 2011, **2**, 2241–2251.
- 31 <https://cmr.fysik.dtu.dk/>.
- 32 B. G. Abreha, S. Agarwal, I. Foster, B. Blaiszik and S. A. Lopez, Virtual Excited State Reference for the Discovery of Electronic Materials Database: An Open-Access Resource for Ground and Excited State Properties of Organic Molecules, *J. Phys. Chem. Lett.*, 2019, **10**, 6835–6841.
- 33 S.-H. Chou, H.-W. Kang, S.-T. Chang, K.-Y. Wu, G. C. Bazan, C.-L. Wang, H.-L. Lin, J.-H. Chang, H.-W. Lin, Y.-C. Huang, C.-S. Tsao and K.-T. Wong, Cofacial Versus Coplanar Arrangement in Centrosymmetric Packing Dimers of Dipolar Small Molecules: Structural Effects on the Crystallization Behaviors and Optoelectronic Characteristics, *ACS Appl. Mater. Interfaces*, 2016, **8**, 18266–18276.
- 34 <https://figshare.com/projects/GuacaMol/56639>.
- 35 N. Brown, M. Fiscato, M. H. Segler and A. C. Vaucher, Guacamol: benchmarking models for de novo molecular design, *J. Chem. Inf. Model.*, 2019, **59**, 1096–1108.
- 36 A. D. Becke, A new mixing of Hartree–Fock and local density-functional theories, *J. Chem. Phys.*, 1993, **98**, 1372–1377.
- 37 K. Raghavachari, Perspective on “Density functional thermochemistry. III. The role of exact exchange”, *Theor. Chem. Acc.*, 2000, **103**, 361–363.
- 38 P. J. Stephens, F. Devlin, C. Chabalowski and M. J. Frisch, Ab initio calculation of vibrational absorption and circular dichroism spectra using density functional force fields, *J. Phys. Chem.*, 1994, **98**, 11623–11627.
- 39 T. Körzdörfer and J.-L. Brédas, Organic Electronic Materials: Recent Advances in the DFT Description of the Ground and Excited States Using Tuned Range-Separated Hybrid Functionals, *Acc. Chem. Res.*, 2014, **47**, 3284–3291.
- 40 S. Maekawa and K. Moorthi, Polymer Optical Constants from Long-Range Corrected DFT Calculations, *J. Phys. Chem. B*, 2016, **120**, 2507–2516.
- 41 S. Riniker and G. A. Landrum, Better informed distance geometry: using what we know to improve conformation generation, *J. Chem. Inf. Model.*, 2015, **55**, 2562–2574.
- 42 A. K. Rappé, C. J. Casewit, K. Colwell, W. A. Goddard III and W. M. Skiff, UFF, a full periodic table force field for molecular mechanics and molecular dynamics simulations, *J. Am. Chem. Soc.*, 1992, **114**, 10024–10035.
- 43 C. Bannwarth, S. Ehlert and S. Grimme, GFN2-xTB—An accurate and broadly parametrized self-consistent tight-binding quantum chemical method with multipole electrostatics and density-dependent dispersion contributions, *J. Chem. Theory Comput.*, 2019, **15**, 1652–1671.
- 44 Y.-S. Lin, G.-D. Li, S.-P. Mao and J.-D. Chai, Long-Range Corrected Hybrid Density Functionals with Improved



- Dispersion Corrections, *J. Chem. Theory Comput.*, 2013, **9**, 263–272.
- 45 F. Neese, Software update: the ORCA program system, version 4.0, *Wiley Interdiscip. Rev.: Comput. Mol. Sci.*, 2018, **8**, e1327.
  - 46 S. Grimme, A simplified Tamm-Dancoff density functional approach for the electronic excitation spectra of very large molecules, *J. Chem. Phys.*, 2013, **138**, 244104.
  - 47 C. Bannwarth and S. Grimme, A simplified time-dependent density functional theory approach for electronic ultraviolet and circular dichroism spectra of very large molecules, *Comput. Theor. Chem.*, 2014, **1040–1041**, 45–53, Excited states: from isolated molecules to complex environments.
  - 48 F. Weigend and R. Ahlrichs, Balanced basis sets of split valence, triple zeta valence and quadruple zeta valence quality for H to Rn: Design and assessment of accuracy, *Phys. Chem. Chem. Phys.*, 2005, **7**, 3297–3305.
  - 49 F. Weigend, Accurate Coulomb-fitting basis sets for H to Rn, *Phys. Chem. Chem. Phys.*, 2006, **8**, 1057–1065.
  - 50 K. Cho, B. Van Merriënboer, C. Gulcehre, D. Bahdanau, F. Bougares, H. Schwenk and Y. Bengio, Learning phrase representations using RNN encoder-decoder for statistical machine translation, arXiv preprint arXiv:1406.1078, 2014.
  - 51 D. P. Kingma and J. Ba, Adam: A method for stochastic optimization, arXiv preprint arXiv:1412.6980, 2014.
  - 52 A. Paszke, S. Gross, S. Chintala, G. Chanan, E. Yang, Z. DeVito, Z. Lin, A. Desmaison, L. Antiga and A. Lerer, *Automatic differentiation in PyTorch. NIPS-W*, 2017.
  - 53 G. Landrum, *RDKit: Open-source cheminformatics*, 2006.
  - 54 V. D. Blondel, J.-L. Guillaume, R. Lambiotte and E. Lefebvre, Fast unfolding of communities in large networks, *J. Stat. Mech.: Theory Exp.*, 2008, **2008**, P10008.
  - 55 K. T. Schütt, P. Kessel, M. Gastegger, K. A. Nicoli, A. Tkatchenko and K.-R. Müller, SchNetPack: A Deep Learning Toolbox For Atomistic Systems, *J. Chem. Theory Comput.*, 2019, **15**, 448–455.
  - 56 C. Chen, W. Ye, Y. Zuo, C. Zheng and S. P. Ong, Graph Networks as a Universal Machine Learning Framework for Molecules and Crystals, *Chem. Mater.*, 2019, **31**, 3564–3572.
  - 57 R. Ramakrishnan, P. O. Dral, M. Rupp and O. A. Von Lilienfeld, Quantum chemistry structures and, properties of 134 kilo molecules, *Sci. Data*, 2014, **1**, 140022.
  - 58 J. L. Durant, B. A. Leland, D. R. Henry and J. G. Nourse, Reoptimization of MDL keys for use in drug discovery, *J. Chem. Inf. Comput. Sci.*, 2002, **42**, 1273–1280.
  - 59 L. v. d. Maaten and G. Hinton, Visualizing data using t-SNE, *J. Mach. Learn. Res.*, 2008, **9**, 2579–2605.
  - 60 P. Ertl and A. Schuffenhauer, Estimation of synthetic accessibility score of drug-like molecules based on molecular complexity and fragment contributions, *J. Cheminf.*, 2009, **1**, 8.
  - 61 P. Politzer, J. Martinez, J. S. Murray and M. C. Concha, An electrostatic correction for improved crystal density predictions of energetic ionic compounds, *Mol. Phys.*, 2010, **108**, 1391–1396.
  - 62 H. Yao, L. Ye, H. Zhang, S. Li, S. Zhang and J. Hou, Molecular design of benzodithiophene-based organic photovoltaic materials, *Chem. Rev.*, 2016, **116**, 7397–7457.
  - 63 S. Chaurasia, C.-Y. Hsu, H.-H. Chou and J. T. Lin, Synthesis, optical and electrochemical properties of pyridal [2,1,3]thiadiazole based organic dyes for dye sensitized solar cells, *Org. Electron.*, 2014, **15**, 378–390.
  - 64 H. Takenaka, T. Ogaki, C. Wang, K. Kawabata and K. Takimiya, Selenium-Substituted  $\beta$ -Methylthiobenzo [1, 2-b:4, 5-b] dithiophenes: Synthesis, Packing Structure, and Transport Properties, *Chem. Mater.*, 2019, **31**, 6696–6705.
  - 65 M. C. Scharber, D. Mühlbacher, M. Koppe, P. Denk, C. Waldauf, A. J. Heeger and C. J. Brabec, Design rules for donors in bulk-heterojunction solar cells—Towards 10% energy-conversion efficiency, *Adv. Mater.*, 2006, **18**, 789–794.
  - 66 R. Gómez-Bombarelli, J. Aguilera-Iparraguirre, T. D. Hirzel, D. Duvenaud, D. Maclaurin, M. A. Blood-Forsythe, H. S. Chae, M. Einzinger, D.-G. Ha, T. Wu, G. Markopoulos, S. Jeon, H. Kang, H. Miyazaki, M. Numata, S. Kim, W. Huang, S. I. Hong, M. Baldo, R. P. Adams and A. Aspuru-Guzik, Design of efficient molecular organic light-emitting diodes by a high-throughput virtual screening and experimental approach, *Nat. Mater.*, 2016, **15**, 1120–1127.
  - 67 H. Bronstein, C. B. Nielsen, B. C. Schroeder and I. McCulloch, The role of chemical design in the performance of organic semiconductors, *Nat. Rev. Chem.*, 2020, 1–12.

